Published in final edited form as:
J Mol Endocrinol. 2013 ; 51(1): 191–202. doi:10.1530/JME-13-0021.

G-protein Coupled Receptor 30 Interacts with Receptor Activity Modifying Protein 3 and Confers Sex-Dependent Cardioprotection

Patricia M. Lenhart[1], **Stefan Broselid**[2], **Cordelia J. Barrick, Ph.D.**[1], **L.M. Fredrik Leeb-Lundberg, Ph.D.**[2], and **Kathleen M. Caron, Ph.D.**[1,*]

[1]Department of Cell Biology & Physiology, The University of North Carolina, Chapel Hill, North Carolina, USA 27599

[2]Department of Experimental Medical Science, Lund University, SE-22184 Lund, Sweden

Abstract

Receptor activity modifying protein 3 (RAMP3) is a single pass transmembrane protein known to interact with and affect the trafficking of several G-protein coupled receptors (GPCRs). We sought to determine whether RAMP3 interacts with G-protein coupled receptor 30 (GPR30), also known as G-protein estrogen receptor 1 (GPER1). GPR30 is a GPCR that binds estradiol and has important roles in cardiovascular and endocrine physiology. Utilizing bioluminescence resonance energy transfer titration studies, co-immunoprecipitation, and confocal microscopy, we show that GPR30 and RAMP3 interact. Furthermore, the presence of GPR30 leads to increased expression of RAMP3 at the plasma membrane in HEK293 cells. *In vivo*, there are marked sex differences in the subcellular localization of GPR30 in cardiac cells, and the hearts of *Ramp3*$^{-/-}$ mice also show signs of GPR30 mislocalization. To determine whether this interaction might play a role in cardiovascular disease, we treated *Ramp3*$^{+/+}$ and *Ramp3*$^{-/-}$ mice on a heart disease-prone genetic background with G-1, a specific agonist for GPR30. Importantly, this *in vivo* activation of GPR30 resulted in a significant reduction in cardiac hypertrophy and perivascular fibrosis that is both RAMP3- and sex-dependent. Our results demonstrate that GPR30-RAMP3 interaction has functional consequences on the localization of these proteins both *in vitro* and *in vivo*, and that RAMP3 is required for GPR30-mediated cardioprotection.

Keywords

G-protein coupled receptors; estradiol; cardiac hypertrophy; cardioprotection

[*]To whom correspondence should be addressed: Kathleen M. Caron, Department of Cell Biology & Physiology, CB # 7545, 6340B MBRB, 111 Mason Farm Road, The University of North Carolina at Chapel Hill, Chapel Hill, North Carolina 27599. Tel: 919-966-5215, Fax: 919-966-5230. kathleen_caron@med.unc.edu.

Declaration of Interest

The authors declare that they have no conflicts of interest.

Author Contributions

PML, SB, and CDB designed and performed experiments and analyzed results. PML wrote the manuscript with input from all coauthors. LMFLL and KMC designed experiments, analyzed data and provided the conceptual framework for the research.

Introduction

Receptor activity modifying proteins (RAMPs), are single-pass, transmembrane accessory proteins that interact with G-protein coupled receptors (GPCRs) to modulate their trafficking, ligand binding specificity, and downstream signaling. The RAMPs were first identified in association with calcitonin receptor-like receptor (CLR) (Bomberger, et al. 2012; McLatchie, et al. 1998)—a discovery which clarified considerable controversy over CLR function and has since been exploited by the pharmaceutical industry for the development of small molecule drugs that specifically target the RAMP-CLR interface (Sexton, et al. 2009). Several additional GPCRs have been shown to interact with RAMPs (Christopoulos, et al. 2003; Harikumar, et al. 2009). Therefore, there remains great interest in understanding the pharmacological and biochemical properties of the RAMPs and in continuing to identify novel GPCR targets for these proteins, with the ultimate goal of manipulating the RAMP-GPCR interface for treatment of human disease.

RAMP3 is unique among the RAMP family members in that it is transcriptionally induced by estradiol (Hewitt, et al. 2005; Watanabe, et al. 2006) and has been shown to play a sex-dependent role in the development of cardiac hypertrophy and transition to heart failure (Barrick, et al. 2012). For these reasons, we considered that GPR30, or G-protein coupled estrogen receptor 1 (GPER1), might be a candidate RAMP3-binding GPCR. GPR30 binds estradiol with high affinity, eliciting rapid intracellular signaling (Carmeci, et al. 1997; Filardo, et al. 2007), and mediates pleiotropic functions in the cardiovascular, endocrine, immune, and central nervous systems (Nilsson, et al. 2011; Olde and Leeb-Lundberg 2009; Prossnitz and Barton 2011).

There is substantial evidence for GPR30-mediated cardioprotection. GPR30 is expressed in the rodent and human heart (Deschamps and Murphy 2009; Patel, et al. 2010), and using male rats, Filice et. al. showed that GPR30 is involved in mediating the effects of estradiol in the heart (Filice, et al. 2009). Numerous studies have explored the effects of pharmacological activation of GPR30 with G-1, a synthetic agonist for GPR30 that specifically activates GPR30 but does not activate the steroid estradiol receptors (Bologa, et al. 2006). Administration of G-1 is directly cardioprotective, reducing infarct size in rat and mouse hearts exposed to ischemia-reperfusion (Bopassa, et al. 2010; Deschamps and Murphy 2009). Furthermore, chronic G-1 treatment reduces left ventricular wall thickness and myocyte hypertrophy without significant effects on blood pressure or fibrosis in a rat model of salt-induced hypertension (Jessup, et al. 2010) and attenuates heart failure (Kang, et al. 2012) and diastolic dysfunction independent of blood pressure in ovariectomized female rats (Wang, et al. 2012). Based on these preclinical studies, pharmacological activation of GPR30 as a potential therapeutic intervention could have utility in the treatment of cardiovascular disease.

Despite what is known about GPR30, there remains intense controversy regarding the trafficking and subcellular localization of GPR30, in addition to many conflicting reports regarding its downstream signaling and even ligand binding specificity. Since RAMPs serve to modulate these aspects of GPCR behavior, we hypothesized that an interaction with RAMPs could potentially clarify some of the controversies surrounding GPR30. Specifically, we sought to determine whether RAMP3, an estradiol-induced accessory protein known to be important in cardiovascular disease, could interact with and modulate the function of GPR30, as an estradiol receptor with protective roles in cardiac and vascular biology.

Materials & Methods

Animals - *Ramp3*$^{-/-}$ animals were generated as previously described (Dackor, et al. 2007) and *Ramp3*$^{+/+}$ and *Ramp3*$^{-/-}$ mice were crossed to heterozygous RenTgMK mice (Barrick et al. 2012). Experimental animals were 8 weeks of age and maintained on an isogenic 129S6/SvEv genetic background. All experiments were approved by the Institutional Animal Care and Use Committee of the University of North Carolina at Chapel Hill.

Bioluminescence Resonance Energy Transfer

BRET titration studies to test the molecular association between GPR30 and RAMP3 were carried out as previously described (Heroux, et al. 2007). Briefly, the calcium phosphate precipitation method was used to transfect HEK293 cells with a constant amount of hGPR30-*R*Luc, hCLR-*R*Luc (positive control), hB2AR-*R*Luc, or hD1R-*R*Luc (negative controls) and increasing doses of hRAMP3-YFP. Cells were treated with the luciferase substrate coelanterazine H for 10 minutes and read using a Berthold Technologies Mithras LB940 plate reader. BRET signal was calculated as the ratio of light emitted from YFP (530 nm) to light emitted from *R*Luc (485 nm). Total fluorescence emission was measured at 530 nm from wells not treated with coelanterazine H that were excited at 485 nm to control for the expression level of hRAMP3-YFP, and total luminescence was determined to control for the expression level of the receptors. Results were analyzed using GraphPad Prism. Results shown are representative of at least three replicate BRET experiments that were performed with similar results.

Co-immunoprecipitation

HEK293 cells were transfected with HA-RAMP3 and FLAG-GPR30 using TransIT-293 (Mirus) and GPR30 was immunoprecipitated by incubating the cleared cell lysates overnight at 4°C with M2 FLAG antibody beads (Sigma-Aldrich). The precipitate was washed extensively and sequentially in lysis buffer and in 10 mM Tris-HCl, pH 7.4. For immunoblotting, proteins were denatured in SDS-polyacrylamide gel electrophoresis sample buffer including 6% β-mercaptoethanol for 30 min at 37°C, fractionated by SDS-polyacrylamide gel electrophoresis, transferred to a nitrocellulose membrane, and the membrane was blocked for at least 45 min in Tris-buffered saline and 10% nonfat milk. The proteins were stained by incubating with rabbit anti-HA antibody (Invitrogen; 1:1000) for 1 hr at room temperature. Immunoreactive bands were visualized with a chemiluminescence kit using anti-rabbit peroxidase-labeled secondary antibody (GE Healthcare) according to the procedure described by the supplier (PerkinElmer Life and Analytical Sciences).

Confocal Imaging

HEK293 cells were transfected with HA-RAMP3 and FLAG-GPR30 using TransIT-293 (Mirus). Transfected cells were grown on glass coverslips coated with poly(D-lysine), and then incubated in serum- and phenol-free media for at least 1 hr at 37°C. For live cell staining, cells were then incubated in serum- and phenol-free media containing IgG1 monoclonal anti-HA (1:100; Covance) and IgG2b monoclonal anti-M1 FLAG (1:500; Sigma-Aldrich) primary antibodies for 30 min at 37°C. Cells were fixed with 3.7% formaldehyde in PBS and permeabilized, then washed with PBS and incubated with anti-IgG1-488 and anti-IgG2b-568 secondary antibodies (Invitrogen). Alternatively, for dead cell staining, cells were incubated with both primary and secondary antibodies after fixation. Cells were also stained with 4',6-diamidino-2-phenylindole (DAPI). Images were collected using a Nikon Eclipse confocal fluorescence microscope (Nikon, Tokyo, Japan) and analyzed with Nikon EC-Z1 3.90 software.

Gene Expression Analysis

mGpr30 and *mRamp3* gene expression was analyzed by quantitative reverse transcription (RT)-PCR with the Applied Biosystems StepOne Plus machine. The primer/probe set for *Ramp3* has been previously described (Dackor et al. 2007). For *Gpr30*, we used a pre-designed Assay on Demand primer/probe set (#Mm02620446_s1, Applied Biosystems). Mouse eukaryotic translation elongation factor 1 alpha 1 was used as the internal control for all samples; the primer/probe set has been previously described (Barrick et al. 2012). RNA was isolated from adult tissues with TRIzol reagent (Life Technologies) and subsequently DNase treated. Two micrograms of total RNA was used to generate cDNA with the MMLV Reverse Transcriptase kit (Life Technologies). The delta–delta Ct method was used to determine the relative levels of gene expression and shown as a fold increase over wildtype male controls. Estrus cycle phase was determined by microscopic examination of mouse vaginal smears stained with the Kwik Diff Stain Kit (Thermo Scientific). For the ovariectomized samples, mice were 21 to 28 days old at the time of ovariectomy. Mice were anesthetized with avertin (0.2–0.4ml/10gm body wt of 1.25% solution) and placed on a warm heating pad to maintain body temperature throughout the surgical procedure. Hair was removed from the abdomen and a small <1 cm incision was made through the abdominal wall about 1 cm to the left of the spinal cord. The ovary was exteriorized and placed on a sterile drape. Silk sutures were used to ligate the oviduct and anterior connective tissue prior to excising the ovary. The body wall was then sutured with dissolvable sutures and wound clips were used to close the skin. The procedure was repeated on the animal's right side. Wound clips are removed 4–5 days after surgery; 4 weeks later the ovariectomized mice were dissected and the heart tissue was used for RT-PCR.

Subcellular Fractionation and Western Blotting

Homogenized lysates were prepared from heart tissue of *Ramp3*$^{+/+}$, *Ramp3*$^{-/-}$, RenTgMK;*Ramp3*$^{+/+}$, and RenTgMK;*Ramp3*$^{-/-}$ male and female mice. The nuclear pellet was removed by centrifuging at 1300x*g* for 1 hr. Membrane-enriched fractions of cardiac lysates were isolated by subsequent ultracentrifugation at 20,000x*g* for 1 hr, and the remaining supernatant was designated as the cytosolic fraction. Lysates were denatured in SDS-polyacrylamide gel electrophoresis sample buffer including 6% β-mercaptoethanol for 5 min at 100°C, fractionated by SDS-polyacrylamide gel electrophoresis, transferred to a nitrocellulose membrane, and the membrane was blocked for 1 hr in casein (ThermoScientific). The membrane was stained using rabbit anti-GPR30 primary antibody (MBL International) or mouse anti-actin (Sigma-Aldrich) as a loading control, followed by goat anti-rabbit 680 or goat anti-mouse 800 secondary antibody (ThermoScientific). Membranes were imaged via LI-COR and quantitation of integrated density normalized to actin was performed using ImageJ. The student's T-test was used to compare the ratio of plasma membrane to cytosolic GPR30 protein relative to actin and a value of $p<0.05$ was considered statistically significant. Results shown are representative of at least three replicate fractionation experiments that were performed with similar results.

G-1 treatment *and* histology

Male and female RenTgMK;*Ramp3*$^{+/+}$ and RenTgMK;*Ramp3*$^{-/-}$ mice at eight weeks of age were anesthetized with avertin (0.2–0.4ml/10gm body wt of 1.25% solution) and injected with a subcutaneous, continuous release pellet (Innovative Research of America) containing six milligrams of G-1 (Tocris) or placebo similar to a previously described method (Wang, et al. 2009). After 40 days of treatment the mice were euthanized. To determine the left ventricle to body weight ratio, the heart chambers were dissected and the left ventricle was weighed. The Mann-Whitney test was used to compare LV:BW data; a value of $p<0.05$ was considered statistically significant. Subsequently, the left ventricle was fixed in 4% paraformaldehyde and 5 μm sections were prepared for staining. Masson's Trichrome

stained slides imaged at 10X were used to analyze interstitial and perivascular cardiac fibrosis. Interstitial fibrosis was quantified by blinded scoring of the extent of interstitial fibrosis in one representative field per mouse. Perivascular fibrosis was quantified by measuring the area of fibrosis surrounding a vessel normalized to the vessel lumen area, using ImageJ software. Three vessels were measured per mouse. Cardiomyocyte area was determined by measuring the cross-sectional area of five cardiomyocytes in each of two fields per mouse from hematoxylin and eosin (H&E) stained slides at 25X, using ImageJ software. For analysis of fibrosis and cardiomyocyte area, the student's T-test was used to compare data and a value of $p<0.05$ was considered statistically significant.

Blood pressure measurements

Male and female RenTgMK;*Ramp3*$^{+/+}$ and RenTgMK;*Ramp3*$^{-/-}$ mice at 2–5 months of age were injected with a subcutaneous, continuous release pellet containing six milligrams of G-1 or placebo as described above. Blood pressures were measured on unanesthetized mice using a Coda computerized volume pressure recording tail cuff system (Kent Scientific). After a five day period of acclimation to the tail cuff system, blood pressures were measured daily for five days on each mouse during the third week following pellet injection. The student's T-test was used to compare data; a value of $p<0.05$ was considered statistically significant.

Results

To directly test whether GPR30 and RAMP3 interact in living cells, we utilized bioluminescence resonance energy transfer (Heroux et al.) titration studies (Heroux et al. 2007). HEK293 cells were transfected with a constant dose of hGPR30-*R*Luc and increasing doses of hRAMP3-YFP. We observed a robust increase in the BRET signal with increasing amounts of hRAMP3 (ΔBRET=0.664), indicating a specific interaction between the two proteins (Figure 1A). Almost no change in BRET signal was seen with the negative controls, B2-adrenergic receptor (ΔBRET=0.061), and Dopamine-1 receptor (ΔBRET=0.079). The positive increase in BRET signal observed for hGPR30 and hRAMP3 was an order of magnitude greater than the negative controls and comparable to that seen with the positive control, hCLR (ΔBRET=0.728).

To further confirm that hGPR30 and hRAMP3 interact, we performed co-immunoprecipitation. In cells transfected with either FLAG-hGPR30 alone or with HA-hRAMP3, we immunoprecipitated with M2-FLAG beads and immunoblotted for HA (Figure 1B). The M2-FLAG beads pull down HA material only when FLAG-hGPR30 and HA-hRAMP3 are co-expressed, indicating by a second technique that GPR30 and RAMP3 interact.

The ability of GPCRs to enhance the localization of RAMPs in the plasma membrane is the standard method in the field by which the association of receptors with RAMPs has been tested (Harikumar et al. 2009). Therefore, we imaged the interaction of GPR30 and RAMP3 by confocal microscopy of HEK293 cells transiently transfected with HA-hRAMP3 and FLAG-hGPR30 and stained with epitope-specific antibodies. The top row of Figure 2A shows cells stained following fixation to identify total cellular proteins. In this representative field, cells are present expressing HA-hRAMP3 alone and together with FLAG-hGPR30. When expressed alone, diffuse RAMP3 staining occurs throughout the cell. On the other hand, co-expression with GPR30 organizes RAMP3 staining and extensive co-localization occurs in the plasma membrane and intracellularly on filamentous structures and in puncta. Figure 2B shows cells stained live and imaged after fixation to identify cell surface proteins. In this representative field, cells are present expressing HA-hRAMP3 and FLAG-hGPR30 individually and together. When expressed alone, RAMP3 is primarily in intracellular

puncta. On the other hand, co-expression with GPR30 increases the relative amount of RAMP3 staining at the cell surface and extensive co-localization occurs. Thus, the formation of a GPR30-RAMP3 complex within the cell increases RAMP3 localization to the plasma membrane.

We next sought to determine whether the interaction of GPR30 and RAMP3 has functional consequences *in vivo*. First, we determined the gene expression levels of *Gpr30* and *Ramp3* in the hearts of wildtype mice. Expression of both *Ramp3* (Figure 3A) and *Gpr30* (Figure 3B) was detected in the hearts of male mice, female mice in diestrus and estrus, and in female mice who have been ovariectomized to deplete endogenous estradiol. For both genes, we observed modest increases in females in estrus compared to diestrus. Ovariectomized females had a statistically significant reduction in both *Gpr30* and *Ramp3* expression compared to intact females in diestrus. Though the differences in expression between males and females in the phases of the estrus cycle are modest, these findings, particularly the reduced gene expression in the ovariectomized females, indicate that cardiac *Gpr30* and *Ramp3* gene expression levels correlate with endogenous estradiol.

Using heart tissue from *Ramp3*$^{+/+}$ and *Ramp3*$^{-/-}$ mice, we investigated GPR30 protein levels and localization by performing subcellular fractionation and western blots for GPR30. In pooled heart lysates (n=3) from *Ramp3*$^{+/+}$ mice, we detected robust expression of GPR30 protein at the expected molecular size (50 kD) in the membrane fraction and very little in the cytosolic fraction (Figure 4A). In contrast, pooled *Ramp3*$^{-/-}$ heart lysates (n=3) showed reduced membrane GPR30 levels (GPR30 integrated density at membrane relative to actin - *Ramp3*$^{-/-}$ = 0.27 compared to *Ramp3*$^{+/+}$ = 1.0). The *Ramp3*$^{-/-}$ hearts also show a concomitant increase in cytosolic GPR30 protein relative to wildtype (Figure 4A). To determine whether cardiac expression and localization of GPR30 protein differs by sex, we performed this same experiment using male and female hearts side-by-side. Figure 4B shows the membrane fraction from these samples. These data show that *Ramp3*$^{+/+}$ hearts have more membrane-localized GPR30 than *Ramp3*$^{-/-}$ hearts in both sexes. Furthermore, female hearts have more overall GPR30 at the membrane compared to males, a difference that was statistically significant for wildtype animals (relative GPR30 integrated density at membrane - females: *Ramp3*$^{+/+}$ = 1.0, *Ramp3*$^{-/-}$ = 0.43; males: *Ramp3*$^{+/+}$ = 0.41, *Ramp3*$^{-/-}$ = 0.10).

To explore the effect of RAMP3 on GPR30 localization in the setting of cardiovascular disease, we utilized RenTgMK mice. The RenTgMK mouse is a well-described model of angiotensin II-mediated chronic hypertension and cardiac hypertrophy (Caron, et al. 2004; Caron, et al. 2002; Caron, et al. 2005). We have previously shown that *Ramp3* gene expression is increased in the hearts of RenTgMK mice of both sexes compared to wildtype, and this heart disease-related upregulation of *Ramp3* is greatest in females (Barrick et al. 2012). For the current study, we generated RenTgMK mice lacking *Ramp3* (RenTgMK;*Ramp*3$^{-/-}$) and RenTgMK mice with intact RAMP3 (RenTgMK;*Ramp3*$^{+/+}$), isolated heart tissue, and performed subcellular fractionation and western blotting to determine GPR30 localization in this model of heart disease. Consistent with our findings in wildtype animals, we detected more GPR30 protein at the membrane in RenTgMK females than in males (relative GPR30 integrated density at membrane - females = 1.0; males = 0.58) (Figure 4C). Using replicate samples, we also observed that RenTgMK;*Ramp*3$^{-/-}$ mice had reduced GPR30 at the plasma membrane compared to RenTgMK;*Ramp3*$^{+/+}$ mice (relative GPR30 integrated density at membrane - RenTgMK;*Ramp3*$^{+/+}$ = 1.0; RenTgMK;*Ramp3*$^{-/-}$ = 0.29) (Figure 4D). Figure 4E summarizes the quantitative findings and statistical analysis from each of these experiments. For both sexes, there is a robust trend of reduced membrane to cytosolic (P:C) ratio of GPR30 protein in disease-free and RenTgMK hearts in the absence of *Ramp3*. Female mice have a higher P:C ratio of GPR30

protein compared to males across all conditions, and this sex difference is statistically significant in *Ramp3*$^{+/+}$ and RenTgMK;*Ramp3*$^{+/+}$ hearts. Thus, female mice have significantly increased membrane-localized GPR30 protein compared to males, and there is a trend of GPR30 protein mislocalization in male and female *Ramp3*$^{-/-}$ and RenTgMK;*Ramp3*$^{-/-}$ heart tissue.

Finally, we investigated whether pharmacological activation of GPR30 is cardioprotective in the RenTgMK model of heart disease, and whether these effects are dependent on RAMP3. We treated male and female RenTgMK;*Ramp3*$^{+/+}$ and RenTgMK;*Ramp*3$^{-/-}$ mice with G-1, the specific agonist for GPR30, or a placebo for a period of 40 days and then performed cardiovascular phenotyping. First, we measured blood pressure to determine whether G-1 treatment affected the hypertensive phenotype of the RenTgMK mice. We found no significant change in blood pressure with G-1 treatment in male (RenTgMK;*Ramp3*$^{+/+}$ placebo = 145.6 ± 22.4 mmHg, RenTgMK;*Ramp3*$^{+/+}$ G-1 = 148.7 ± 25.9 mmHg; RenTgMK;*Ramp3*$^{-/-}$ placebo = 150.3 ± 38.6 mmHg, RenTgMK;*Ramp3*$^{-/-}$ G-1 = 159.5 ± 25.1 mmHg) or female mice (RenTgMK;*Ramp3*$^{+/+}$ placebo = 128.5 ± 25.6 mmHg, RenTgMK;*Ramp3*$^{+/+}$ G-1 = 118.0 ± 25.0 mmHg; RenTgMK;*Ramp3*$^{-/-}$ placebo = 135.8 ± 27.4 mmHg, RenTgMK;*Ramp3*$^{-/-}$ G-1 = 140.1 ± 38.8 mmHg).

Next, we examined cardiac fibrosis. Consistent with other studies (Jessup et al. 2010), we found that there were no overt differences in interstitial fibrosis between the genotypes or with G-1 treatment in male mice (Figure 5A and B). However, G-1 treatment did result in a statistically significant reduction in perivascular fibrosis (Figure 5C and D) in the hearts of RenTgMK;*Ramp3*$^{+/+}$, but not RenTgMK;*Ramp*3$^{-/-}$, male mice. We also examined female hearts and found no significant differences in either perivascular or interstitial fibrosis.

We also found interesting changes in the left ventricle to body weight (LV:BW) ratio of these mice. The LV:BW ratio of RenTgMK;*Ramp3*$^{+/+}$ male mice was significantly reduced with G-1 treatment compared to placebo (Figure 6A). RenTgMK;*Ramp*3$^{-/-}$ males, on the other hand, had no reduction in their left ventricle to body weight ratio with G-1 treatment. Female mice of both genotypes had no significant response to G-1 treatment. Body weights did not differ by genotype or treatment condition for males (RenTgMK;*Ramp3*$^{+/+}$ placebo = 24.36 ± 4.19 g, RenTgMK;*Ramp3*$^{+/+}$ G-1 = 23.79 ± 2.98 g; RenTgMK;*Ramp3*$^{-/-}$ placebo = 23.19 ± 2.73 g, RenTgMK;*Ramp3*$^{-/-}$ G-1 = 23.96 ± 3.39 g) or females (RenTgMK;*Ramp3*$^{+/+}$ placebo = 18.44 ± 1.60 g, RenTgMK;*Ramp3*$^{+/+}$ G-1 = 19.23 ± 2.21 g; RenTgMK;*Ramp3*$^{-/-}$ placebo = 20.05 ± 1.77 g, RenTgMK;*Ramp3*$^{-/-}$ G-1 = 20.15 ± 1.75 g). In addition to determining LV:BW ratios, we measured cardiomyocyte cross-sectional area, which revealed results consistent with the heart weight findings. Only male RenTgMK mice with intact *Ramp3* showed a significant reduction in cardiomyocyte area with G-1 treatment, while females or males lacking *Ramp3* did not respond to G-1 treatment (Figure 6B and C).

Discussion

The identification of novel GPCR-RAMP interactions is of great interest because this complex forms a pharmacologically tractable interface, which could potentially be manipulated for the treatment of human disease (Sexton et al. 2009). In the current study, we identify GPR30, an estradiol receptor with important functions in the cardiovascular system (Nilsson et al. 2011; Olde and Leeb-Lundberg 2009; Prossnitz and Barton 2011), as a novel target for RAMP3, a modifying protein also known for its sex-dependent cardioprotective effects (Barrick et al. 2012). The association of GPR30 with a RAMP is of particular interest because this has the potential to clarify much of the controversy that still surrounds GPR30's

cellular localization, ligand-binding, and function. Furthermore, GPR30 is the first Family A GPCR to be shown to interact with a RAMP.

In the present study, we have made use of both standard and newly available techniques in the field to provide compelling evidence for the GPR30-RAMP3 interaction. Bioluminescence resonance energy transfer, already well-described for its utility in testing protein-protein interactions in general, has recently been used as an elegant and quantitative method to interrogate GPCR-RAMP interactions (Harikumar et al. 2009; Heroux et al. 2007). Here, we use this method to reveal a robust interaction between GPR30 and RAMP3 that is equivalent to that observed with CLR, the canonical RAMP-associated receptor. Co-immunoprecipitation of the epitope tagged GPR30 and RAMP3 proteins further supports this conclusion. In the past, the use of confocal microscopy to test the ability of GPCRs to enhance the localization of RAMPs in the plasma membrane was the standard method by which the association of receptors with RAMPs had been tested (Harikumar et al. 2009). Similarly, with this technique, we found that GPR30 and RAMP3 colocalize, and expression of GPR30 enhances RAMP3 localization to the cell surface. This provides further evidence for an interaction between the two proteins, and shows that the association of GPR30 and RAMP3 alters the localization of this complex.

In addition to the localization effects observed *in vitro*, RAMP3 may also affect localization of GPR30 *in vivo*, as absence of RAMP3 results in a trend of mislocalized GPR30 in both normal mouse heart tissue and in heart tissue on a background of cardiovascular disease. Sex-differences in GPR30 localization were also observed, as the hearts of female mice have a significantly increased proportion of GPR30 protein at the plasma membrane compared to males when *Ramp3*, an estrogen regulated gene, is present. Most importantly, these *in vivo* differences have functional consequences, since pharmacological activation of GPR30 reduces cardiac hypertrophy and perivascular fibrosis in male mice with intact *Ramp3*, while genetic loss of *Ramp3* eliminates this cardioprotective effect. These effects were independent of blood pressure, which is consistent with previous studies showing that chronic G-1 treatment does not affect blood pressure under hypertensive conditions in intact male or female rats (Jessup et al. 2010; Lindsey, et al. 2009; Lindsey, et al. 2011; Wang et al. 2012). Thus, it is likely that this cardioprotection is due to direct effects of GPR30-RAMP3 function in the heart, which is influenced by the localization of the protein complex.

Interestingly, we found that the reduction of cardiac hypertrophy and perivascular fibrosis is only observed in male mice, indicating that protective effect of GPR30 in the heart is both RAMP3- and sex-dependent. Our previously published work has demonstrated that RenTgMK;*Ramp3*$^{-/-}$ males at 5–6 months of age have exacerbated cardiac hypertrophy. We intentionally performed our cardiovascular phenotyping experiments in mice beginning at 2 months of age, and as expected at this early time point, the LV:BW ratios and cardiomyocyte areas did not differ in mice lacking *Ramp3*. Thus, *Ramp3* genotype-dependent effects do not confound the interpretation of our results from the G-1 treatment experiments. Figure 7 models our proposed explanation for why the effectiveness of G-1 treatment was dependent on sex and *Ramp3* genotype. We hypothesize that because female mice have increased GPR30 at the cell membrane compared to males and high levels of the endogenous GPR30 ligand, estradiol, they remain cardioprotected even when *Ramp3* is absent, regardless of G-1 treatment. However, males have reduced membrane GPR30 and low estradiol levels. This leads to a worsened cardiovascular phenotype that can be ameliorated with G-1 treatment only if the males express *Ramp3*, which may maintain GPR30 localization at the cell membrane, allowing for efficient response to ligand treatment. The requirement of intact *Ramp3* for GPR30 cardioprotection may also depend on RAMP-mediated effects in addition to localization, such as downstream signaling. Future

studies will be directed at determining whether and how RAMP3 alters GPR30-mediated cell signaling.

Our results are consistent with our previous studies showing a sex-dependent cardioprotective role for RAMP3 (Barrick et al. 2012), and our findings also complement studies by others including Jessup et. al. showing that G-1 treatment significantly reduces cardiomyocyte hypertrophy in intact females rats with salt-sensitive hypertension (Jessup et al. 2010). Though G-1 treatment reduces interstitial fibrosis in ovariectomized female rats (Kang et al. 2012; Wang et al. 2012), the reduction in perivascular fibrosis with G-1 treatment in male mice shown here is unique. To our knowledge, this is the first report of GPR30 agonist-induced cardioprotection in a genetic mouse model of cardiovascular disease, with the additional discovery of sex differences. The requirement for RAMP3 to mediate these effects is entirely novel.

Our results demonstrate for the first time that GPR30 and RAMP3 interact. This interaction has functional consequences on the localization of these proteins, and we show that RAMP3 plays a critical and sex-dependent role in GPR30-mediated cardioprotection. GPR30-RAMP3 is a novel pathway that may contribute to sex differences in cardiovascular disease susceptibility and progression, and ultimately, this pathway could potentially be targeted for sex-tailored treatment for cardiovascular disease.

Acknowledgments

The authors thank James Barwell, Dan Rathbone, and David Poyner for their helpful discussions and insight. The authors also thank Manyu Li for assistance with cloning, and Kim Fritz-Six and Mahita Kadmiel for assistance with experiments.

Funding

This work was supported by funds from the National Institutes of Health (NIH/NHLBI HL091973 and NIH/NICHD HD060860 to KMC and F30HL104778 to PML), an American Heart Association Established Investigator Award (to KMC), the Swedish Research Council (VR2009-4077 to LMFLL), the Swedish Cancer Society (CAN2011/628 to LMFLL), and the Swedish Research School for Drug Science FLÄK to SB.

References

Barrick CJ, Lenhart PM, Dackor RT, Nagle E, Caron KM. Loss of receptor activity-modifying protein 3 exacerbates cardiac hypertrophy and transition to heart failure in a sex-dependent manner. J Mol Cell Cardiol. 2012; 52:165–174. [PubMed: 22100352]

Bologa CG, Revankar CM, Young SM, Edwards BS, Arterburn JB, Kiselyov AS, Parker MA, Tkachenko SE, Savchuck NP, Sklar LA, et al. Virtual and biomolecular screening converge on a selective agonist for GPR30. Nat Chem Biol. 2006; 2:207–212. [PubMed: 16520733]

Bomberger JM, Parameswaran N, Spielman WS. Regulation of GPCR trafficking by RAMPs. Adv Exp Med Biol. 2012; 744:25–37. [PubMed: 22434105]

Bopassa JC, Eghbali M, Toro L, Stefani E. A novel estrogen receptor GPER inhibits mitochondria permeability transition pore opening and protects the heart against ischemia-reperfusion injury. Am J Physiol Heart Circ Physiol. 2010; 298:H16–23. [PubMed: 19880667]

Carmeci C, Thompson DA, Ring HZ, Francke U, Weigel RJ. Identification of a gene (GPR30) with homology to the G-protein-coupled receptor superfamily associated with estrogen receptor expression in breast cancer. Genomics. 1997; 45:607–617. [PubMed: 9367686]

Caron KM, James LR, Kim HS, Knowles J, Uhlir R, Mao L, Hagaman JR, Cascio W, Rockman H, Smithies O. Cardiac hypertrophy and sudden death in mice with a genetically clamped renin transgene. Proc Natl Acad Sci U S A. 2004; 101:3106–3111. [PubMed: 14978280]

Caron KM, James LR, Kim HS, Morham SG, Sequeira Lopez ML, Gomez RA, Reudelhuber TL, Smithies O. A genetically clamped renin transgene for the induction of hypertension. Proc Natl Acad Sci U S A. 2002; 99:8248–8252. [PubMed: 12034874]

Caron KM, James LR, Lee G, Kim HS, Smithies O. Lifelong genetic minipumps. Physiol Genomics. 2005; 20:203–209. [PubMed: 15585607]

Christopoulos A, Christopoulos G, Morfis M, Udawela M, Laburthe M, Couvineau A, Kuwasako K, Tilakaratne N, Sexton PM. Novel receptor partners and function of receptor activity-modifying proteins. J Biol Chem. 2003; 278:3293–3297. [PubMed: 12446722]

Dackor R, Fritz-Six K, Smithies O, Caron K. Receptor activity-modifying proteins 2 and 3 have distinct physiological functions from embryogenesis to old age. J Biol Chem. 2007; 282:18094–18099. [PubMed: 17470425]

Deschamps AM, Murphy E. Activation of a novel estrogen receptor, GPER, is cardioprotective in male and female rats. Am J Physiol Heart Circ Physiol. 2009; 297:H1806–1813. [PubMed: 19717735]

Filardo E, Quinn J, Pang Y, Graeber C, Shaw S, Dong J, Thomas P. Activation of the novel estrogen receptor G protein-coupled receptor 30 (GPR30) at the plasma membrane. Endocrinology. 2007; 148:3236–3245. [PubMed: 17379646]

Filice E, Recchia AG, Pellegrino D, Angelone T, Maggiolini M, Cerra MC. A new membrane G protein-coupled receptor (GPR30) is involved in the cardiac effects of 17beta-estradiol in the male rat. J Physiol Pharmacol. 2009; 60:3–10. [PubMed: 20065491]

Harikumar KG, Simms J, Christopoulos G, Sexton PM, Miller LJ. Molecular Basis of Association of Receptor Activity-Modifying Protein 3 with the Family B G Protein-Coupled Secretin Receptor. Biochemistry. 2009; 49:11773–85. [PubMed: 19886671]

Heroux M, Breton B, Hogue M, Bouvier M. Assembly and signaling of CRLR and RAMP1 complexes assessed by BRET. Biochemistry. 2007; 46:7022–7033. [PubMed: 17503773]

Hewitt SC, Collins J, Grissom S, Deroo B, Korach KS. Global uterine genomics in vivo: microarray evaluation of the estrogen receptor alpha-growth factor cross-talk mechanism. Mol Endocrinol. 2005; 19:657–668. [PubMed: 15528273]

Jessup JA, Lindsey SH, Wang H, Chappell MC, Groban L. Attenuation of salt-induced cardiac remodeling and diastolic dysfunction by the GPER agonist G-1 in female mRen2.Lewis rats. PLoS One. 2010; 5:e15433. [PubMed: 21082029]

Kang S, Liu Y, Sun D, Zhou C, Liu A, Xu C, Hao Y, Li D, Yan C, Sun H. Chronic activation of the g protein-coupled receptor 30 with agonist g-1 attenuates heart failure. PLoS One. 2012; 7:e48185. [PubMed: 23110207]

Lindsey SH, Cohen JA, Brosnihan KB, Gallagher PE, Chappell MC. Chronic treatment with the G protein-coupled receptor 30 agonist G-1 decreases blood pressure in ovariectomized mRen2.Lewis rats. Endocrinology. 2009; 150:3753–3758. [PubMed: 19372194]

Lindsey SH, Yamaleyeva LM, Brosnihan KB, Gallagher PE, Chappell MC. Estrogen receptor GPR30 reduces oxidative stress and proteinuria in the salt-sensitive female mRen2.Lewis rat. Hypertension. 2011; 58:665–671. [PubMed: 21844484]

McLatchie LM, Fraser NJ, Main MJ, Wise A, Brown J, Thompson N, Solari R, Lee MG, Foord SM. RAMPs regulate the transport and ligand specificity of the calcitonin-receptor-like receptor. Nature. 1998; 393:333–339. [PubMed: 9620797]

Nilsson BO, Olde B, Leeb-Lundberg LM. G protein-coupled oestrogen receptor 1 (GPER1)/GPR30: a new player in cardiovascular and metabolic oestrogenic signalling. Br J Pharmacol. 2011; 163:1131–1139. [PubMed: 21250980]

Olde B, Leeb-Lundberg LM. GPR30/GPER1: searching for a role in estrogen physiology. Trends Endocrinol Metab. 2009; 20:409–416. [PubMed: 19734054]

Patel VH, Chen J, Ramanjaneya M, Karteris E, Zachariades E, Thomas P, Been M, Randeva HS. G-protein coupled estrogen receptor 1 expression in rat and human heart: Protective role during ischaemic stress. Int J Mol Med. 2010; 26:193–199. [PubMed: 20596598]

Prossnitz ER, Barton M. The G-protein-coupled estrogen receptor GPER in health and disease. Nat Rev Endocrinol. 2011; 7:715–726. [PubMed: 21844907]

Sexton PM, Poyner DR, Simms J, Christopoulos A, Hay DL. Modulating receptor function through RAMPs: can they represent drug targets in themselves? Drug Discov Today. 2009; 14:413–419. [PubMed: 19150656]

Wang C, Dehghani B, Li Y, Kaler LJ, Proctor T, Vandenbark AA, Offner H. Membrane estrogen receptor regulates experimental autoimmune encephalomyelitis through up-regulation of programmed death 1. J Immunol. 2009; 182:3294–3303. [PubMed: 19234228]

Wang H, Jessup JA, Lin MS, Chagas C, Lindsey SH, Groban L. Activation of GPR30 attenuates diastolic dysfunction and left ventricle remodelling in oophorectomized mRen2.Lewis rats. Cardiovasc Res. 2012; 94:96–104. [PubMed: 22328091]

Watanabe H, Takahashi E, Kobayashi M, Goto M, Krust A, Chambon P, Iguchi T. The estrogen-responsive adrenomedullin and receptor-modifying protein 3 gene identified by DNA microarray analysis are directly regulated by estrogen receptor. J Mol Endocrinol. 2006; 36:81–89. [PubMed: 16461929]

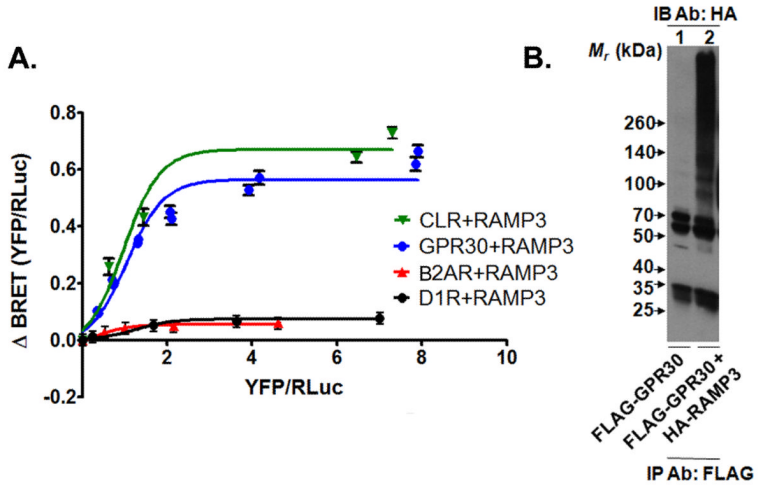

Figure 1. ***In vitro*** **analysis of GPR30-RAMP3 protein-protein interaction**

(A) BRET analysis of the hGPR30-hRAMP3 interaction. hGPR30+hRAMP3 (blue) shows a robust increase in BRET signal with increasing doses of hRAMP3-YFP, as does the positive control, hCLR+ hRAMP3 (green). The negative controls, B2-adrenergic receptor (hB2AR, red), and Dopamine-1 receptor (D1R, black), which are not expected to interact with RAMPs, show negligible change in the BRET signal. Results shown are representative of at least three replicate experiments that were performed with similar results. **(B)** Immunoprecipitation with M2 FLAG beads and immunoblotting with anti-HA primary antibody. M2 FLAG pulls down HA immunoreactivity specifically when FLAG-hGPR30 and HA-hRAMP3 are co-expressed. Non-specific bands at 25 and 50 kDa are IgG bands. The experiment was repeated three times with similar results.

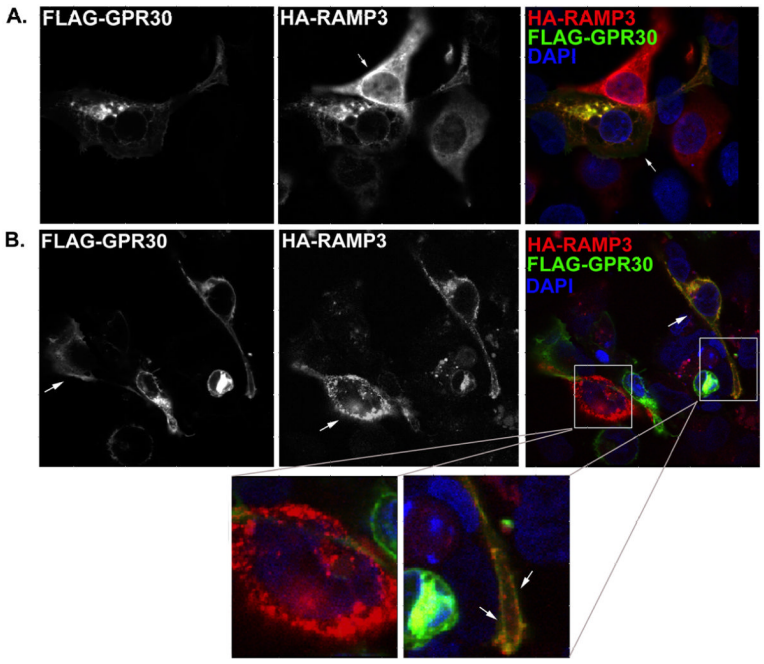

Figure 2. Localization of GPR30 and RAMP3 *in vitro*

(A) Fixed Cell Staining - Confocal microscopy of HEK293 cells transfected with HA-hRAMP3 (green in merged panel) and FLAG-hGPR30 (red in merged panel) stained fixed with M1 FLAG antibody and anti-HA antibody and then with secondary antibody. Left panel shows the FLAG-hGPR30 channel alone, the middle panel shows the HA-hRAMP3 channel alone (arrow indicates a cell expressing only HA-hRAMP3), and the right panel shows the two channels merged with DAPI nuclear stain in blue (arrow indicates a cell expressing both FLAG-hGPR30 and HA-hRAMP3). **(B)** Live Cell Staining - HEK293 cells were similarly transfected and stained live with M1 FLAG antibody and anti-HA antibody followed by fixing and staining with secondary antibody. The left panel shows the FLAG-hGPR30 channel alone (arrow indicates a cell expressing only FLAG-hGPR30, the middle panel shows the HA-hRAMP3 channel alone (arrow indicates a cell expressing only HA-hRAMP3), and the right panel shows the two channels merged with DAPI nuclear stain in blue (arrow indicates a cell expressing both FLAG-hGPR30 and HA-hRAMP3). The regions indicated by the white box are enlarged in the corresponding panels below and arrows indicated colocalization at the plasma membrane. The experiment was repeated three times with similar results.

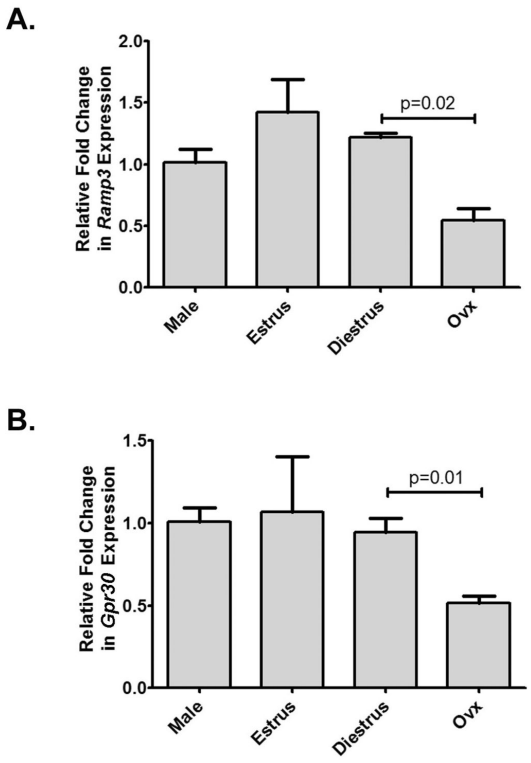

Figure 3. Cardiac Expression of *Gpr30* and *Ramp3*

Quantitative PCR was used to compare the expression of **(A)** *Ramp3* and **(B)** *Gpr30* in the hearts of male mice, female mice in estrus or diestrus, and ovariectomized (Ovx) females; n=3–4 animals per group. Depletion of endogenous estradiol by ovariectomy in female mice results in a statistically significant reduction in expression of both *Ramp3* and *Gpr30* in the heart.

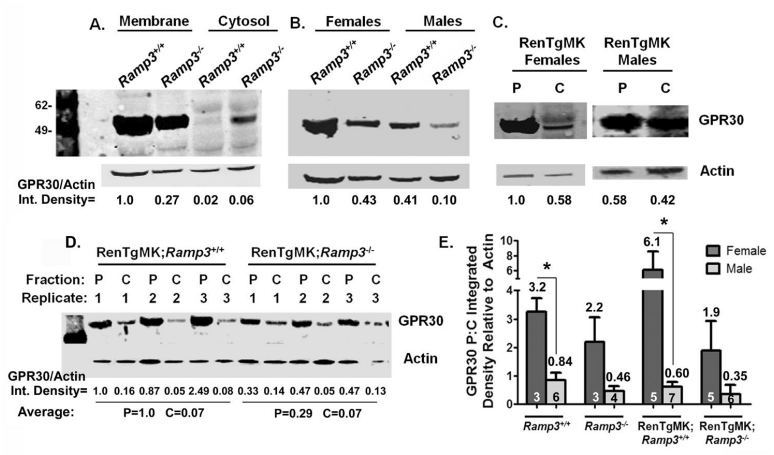

Figure 4. Localization of GPR30 and RAMP3 *in vivo*

(**A**–**D**) GPR30 immunoblots of fractionated cardiac lysates. Membrane-enriched and cytosolic fractions were prepared by ultracentrifugation and western blotting for GPR30 protein was performed. The integrated density of GPR30 normalized to actin for each lane is listed below each blot, with the first lane set equal to 1.0. **(A)** GPR30 western blot of cardiac lysates of *Ramp3*$^{+/+}$ and *Ramp3*$^{-/-}$ mice (n=3 animals per genotype). GPR30 is reduced in the membrane fraction and increased in the cytosolic fraction in *Ramp3*$^{-/-}$ versus *Ramp3*$^{+/+}$ hearts. **(B)** GPR30 western blot of the plasma membrane fraction of cardiac lysates from male and female *Ramp3*$^{+/+}$ and *Ramp3*$^{-/-}$ mice (n=3 animals per group). Females have more membrane-localized GPR30 than males, and loss of *Ramp3* reduces membrane GPR30 levels in both sexes. **(C)** Western blot of the plasma membrane (P) and cytocolic **(C)** fractions of pooled RenTgMK male and female hearts (n=3 animals per group). In this heart disease model, females have increased membrane-localized GPR30 compared to males. **(D)** Western blot of the plasma membrane (P) and cytoplasmic **(C)** fractions of cardiac lysates from replicate samples of RenTgMK;*Ramp3*$^{+/+}$ (n=3) and RenTgMK;*Ramp3*$^{-/-}$ (n=3) mice. Each replicate number represents a separate animal. The average densities for the P and C fraction for each genotype are listed below the blot. Loss of *Ramp3* on the RenTgMK background reduces plasma membrane GPR30. **(E)** Quantitation of immunoblot data showing the normalized ratio of GPR30 protein in the plasma membrane and cytosolic fractions (P:C) in males and female hearts across genotypes. *Ramp3*$^{+/+}$ and RenTgMK;*Ramp3*$^{+/+}$ females have significantly higher GPR30 P:C ratios compared to males of the same genotype. Numbers inside bars represent n for each group, numbers above bars represent the average P:C ratio for each group; * = $p<0.05$.

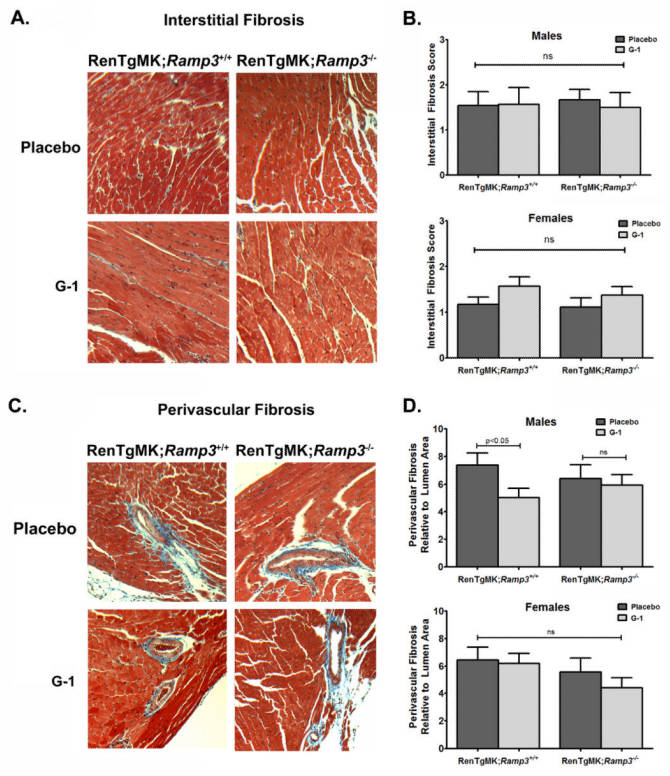

Figure 5. The effect of *in vivo* activation of GPR30 on cardiac fibrosis

(A) Masson's Trichrome staining of interstitial fibrosis in the left ventricle of male RenTgMK;*Ramp3*$^{+/+}$ and RenTgMK;*Ramp3*$^{-/-}$ mice treated with 6 mg continuous release pellets of G-1 or placebo for 40 days, **(B)** with quantitation. No overt differences in interstitial fibrosis were observed between the genotypes or with G-1 treatment. **(C)** Masson's Trichrome staining of perivascular fibrosis in the left ventricle of male RenTgMK;*Ramp3*$^{+/+}$ and RenTgMK;*Ramp3*$^{-/-}$ mice treated with G-1 or placebo, **(D)** with quatitation. G-1 treatment resulted in a statistically significant reduction in perivascular fibrosis in RenTgMK;*Ramp3*$^{+/+}$ males, but not in RenTgMK;*Ramp3*$^{-/-}$ males or female mice of either genotype. N=5–9 animals per group.

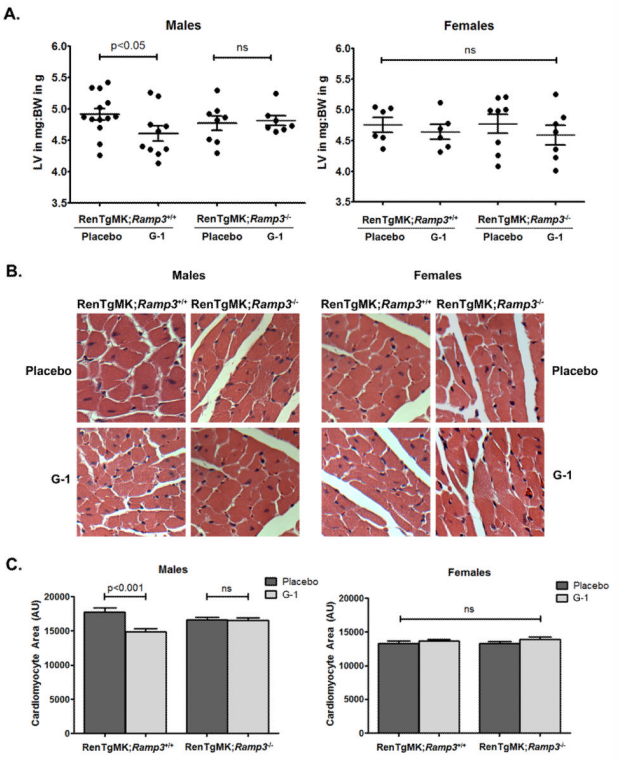

Figure 6. The effect of *in vivo* activation of GPR30 on left ventricular hypertrophy

(A) Left ventricle to body weight (LV:BW) ratios of male and female RenTgMK;*Ramp3*$^{+/+}$ and RenTgMK;*Ramp3*$^{-/-}$ mice treated with the G-1 or placebo. Male RenTgMK;*Ramp3*$^{+/+}$ mice show a statistically significant reduction in LV:BW ratio with G-1 treatment ($p<0.05$). **(B)** Hematoxylin and eosin staining of the left ventricles of male and female RenTgMK;*Ramp3*$^{+/+}$ and RenTgMK;*Ramp3*$^{-/-}$ mice. **(C)** Cardiomyocyte cross-sectional area measurements of male and female RenTgMK;*Ramp3*$^{+/+}$ and RenTgMK;*Ramp3*$^{-/-}$ mice. Male RenTgMK;*Ramp3*$^{+/+}$ mice show a statistically significant reduction in cardiomyocyte area with G-1 treatment ($p<0.001$). N=5–9 animals per group.

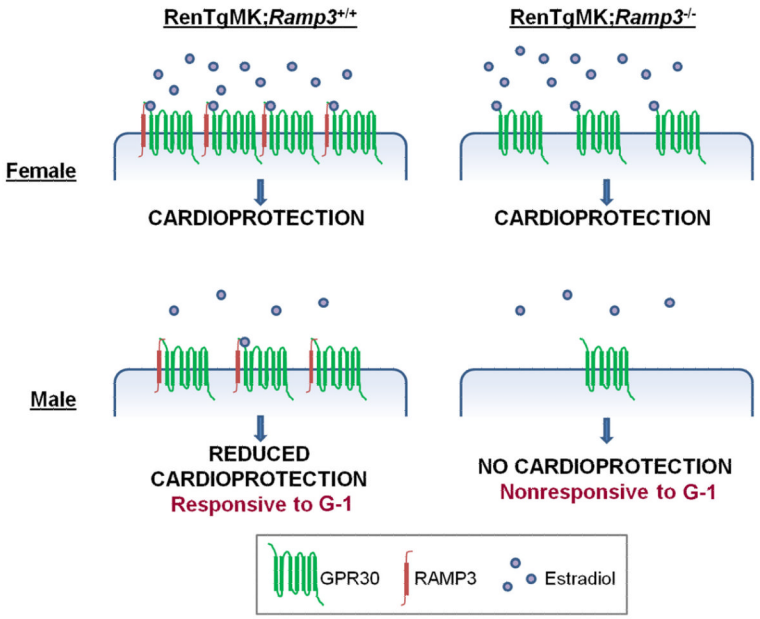

Figure 7. A model of GPR30- and RAMP3-mediated cardioprotection

Female mice have increased GPR30 at the cell membrane compared to males and high levels of the estradiol. Therefore, regardless of G-1 treatment, females may remain cardioprotected even when *Ramp3* is absent. Males have reduced membrane GPR30 and low estradiol levels, and thus lack the natural cardioprotection seen in females. G-1 treatment can improve the cardiovascular phenotype only if the male expresses *Ramp3*, which may maintain GPR30 localization at the cell membrane, allowing for efficient response to ligand treatment.